CGU HS Committee on River Ice Processes and the Environment
14th Workshop on the Hydraulics of Ice Covered Rivers
Quebec City, June 19 - 22, 2007

Numerical study of Ice Conditions, Ice Dynamics and Ice Pressure Events near the Gros Cacouna Site in the St. Lawrence Estuary (winters 1996/97 through 2002/03)

Simon Senneville, M.Sc., François Saucier, Ph.D.
Institut des Sciences de la Mer de Rimouski (ISMER)
Université du Québec à Rimouski
310 Allée des Ursulines,
Rimouski, QC, G5L 3A1, Canada

Brian Wright, M.Sc.
B. Wright & Associates Ltd.
212 Carey
Canmore, Alberta, Canada
T1W 2R6

And

Jorgito Tseng
Sandwell Engineering Inc.
Suite 600 – 885 Dunsmuir Street
Vancouver, BC, Canada
V6C 1N5

Table of Contents

Table of Contents **2**
1.0 Introduction **3**
2.0 Objectives & Approach **3**
3.0 Modelling Method **4**
3.1 General 4
3.2 Some Modelling Details 4
3.2.1 Ocean Model 4
3.2.2 Ice Model 5
3.2.3 Numerical Grid 5
3.2.4 Model Inputs 6
3.3 Initial Conditions 7
3.4 Model Simulation Runs 7
4. 0 Model Solutions **8**
4.1 General 8
4.2 Time Series Displays 9
5.0 Analysis & Results **11**
5.1 General 11
5.2 Frequency of Ice Pressure Events 11
5.2.1 Initial Screening 11
5.2.2 Definition of Thresholds 12
5.2.3 Other Factors 12
5.2.4 Frequency Statistics 12
5.3 Characteristics of Ice Pressure Events 14
5.3. 1 Durations 14
5.3.2 Frequency of events 15
5.3.3 Spatial structures 15
5.4 Causes of Ice Pressure Events 19
6.0 Conclusions **21**
7.0 References **23**

Acknowledgment

This work was commissioned by Cacouna Energy and their permission to publish is gratefully acknowledge.

1.0 Introduction

During the winter period, the St. Lawrence River and Gulf of St. Lawrence are covered by ice. Because many decades of experience have been gathered with vessel transits through the Gulf of St. Lawrence and St. Lawrence River in winter, the ice data base that is available for general region is quite good (Wright and Masterson, 2004). At Gros Cacouna, the site proposed by Cacouna Energy for an LNG terminal, however, the level of ice information is more limited, particularly in terms of some of the site-specific ice parameters needed for various terminal design and operability considerations. In view of this, a number of new studies were initiated over the 2004/05 winter period to obtain better ice information at and around the proposed LNG terminal site. They included several field programs (Koutitonsky et al, 2005; Fissel et al, 2005; Wright, 2005; and Wright and Tseng, 2005), and a model-based hindcast study of ice conditions, ice movements and ice pressure events at the location over a longer time period (7 years), which is the subject of this study.

Figure 1.1: Geographical reference map showing the Gros Cacouna location.

In the following sections, the coupled ice and ocean modelling method that was used to hindcast ice conditions in the upper St. Lawrence Estuary is described, and the key results of the study provided. Here, it should be noted that the main focus of the study has been directed towards the definition of ice pressure events in the immediate vicinity of the Gros Cacouna site.

2.0 Objectives & Approach

The primary objective of this study is provide information about ice pressure events near the Gros Cacouna terminal site, based on simulations made with a detailed coupled sea ice - ocean circulation model for the upper St. Lawrence Estuary, applied in a hindcast mode.

In order to generate reasonably representative statistics about ice pressure events, the model was used to identify ice pressure occurrences over seven winter periods, from 1996/97 to 2000/03.

A step-wise approach has been taken in this study. The key tasks that were undertaken in the study are briefly highlighted as follows.

- Set-up a high resolution (400m) ice/ocean model for the Gros Cacouna terminal area, embedded within a lower resolution (5 km) grid model for downstream St. Lawrence estuary region, for use in a hindacast mode at time scales of 30 seconds for the ocean component and 5 minutes for the ice component.

- Once validated, use the high resolution model to simulate ice conditions across the high resolution grid, with the aim of identifying and quantifying 100 significant ice pressure events over the 7 winters from 1996/97 to 2002/03.

- Assess the resultant ice pressure event data obtained from the modelling study, develop relevant ice pressure statistics from the model outputs, and investigate the primary factors that give rise to ice pressure events in the Gros Cacouna terminal area.

3.0 Modelling Method

3.1 General

In basic terms, the overall model used in this study includes an 3D baroclinic ocean model coupled to an elastic-viscous-plastic ice dynamics model, with surface forcing provided by an atmospheric model. Prior to this study, the various model components had been developed to address similar problem areas to those of interest here. However, they all involved different scales and had not been jointly configured into the high resolution numerical grid required for this study. A description of the key model components and the high resolution numerical grid that has been used in this study is given below, along with some comments about the main input parameters and forcing fields (e.g.: winds) to the model.

3.2 Some Modelling Details

The two main elements of the overall model that has been configured to hindcast ice conditions, ice movements and ice pressure events in this study are its ocean circulation and ice dynamics components. If the model was being used in a forecasting mode, an atmospheric component could also be coupled to it, as the third main element. Also, if simulations were carried out over longer time frames than the ones undertaken here (i.e.: weeks to months versus days), various thermodynamics factors related to ice growth would be incorporated and turned on in the overall model. Note that a lack of computer power precludes such approach at present.

3.2.1 Ocean Model

The ocean model is similar to the one used to produce the "Atlas of Tidal Currents: St. Lawrence Estuary from Cap de Bon-Désir to Trois-Rivières". This atlas has been published by the Canadian Hydrographic Service (Saucier et al, 1999) and is now being routinely used by mariners. Hence, the ocean model (used here) has been well validated (see also Saucier and Chassé, 2000).

This numerical model incorporates all of the key factors, ranging from actual bathymetry, though density and tidal effects, to water run-off from tributary rivers into the St. Lawrence. The model uses a fully prognostic z - level, hydrostatic, shallow water, incompressible formulation from Backhaus (1983; 1985), Stronach et al. (1993), and Saucier et al. (2003). This formulation

provides a hydrostatic solution to mass, momentum and density conservation in the Boussinesq approximations with finite differences. The model makes use of a semi-implicit solution for surface elevations, a flux-corrected transport scheme for scalars (Zalezak, 1979), small horizontal mixing, and a second moment turbulent energy model (e.g., Mellor and Yamada, 1982) using the stability functions from Canuto et al. (2001). The energy part of the model is supplemented with a diagnostic equation for the turbulent master length scale (the minimum of the parabolic law of the wall and the Ozmidov length scales).

3.2.2 Ice Model

In earlier studies, a numerical ice model was developed to forecast ice conditions and movements in the Gulf of St. Lawrence and St. Lawrence River regions. It includes a dynamic (Hunke and Dukowicz, 1997) and thermodynamic (Semtner, 1976) two-layer sea ice model, with the ice thickness distribution following Thorndike et al (1975), and a 1 layer snow cover representation. This numerical ice model has been coupled with an ocean circulation component, on a grid scale of 5 km. Various aspects of this coupled model and some of its previous applications are described in Saucier et al. (2003) and Saucier et al. (2004).
This overall sea ice - ocean model allows the prediction of ice conditions, movements and ice pressure occurrences on short time scales (tens of seconds) during the ice covered period. In this regard, it is important to note that the 5 km grid scale version (including an atmospheric component) is now being used to provide ice forecasts for the Canadian Coast Guard in the Gulf of St. Lawrence and St. Lawrence River areas on an operational basis (e.g., Pellerin et al., 2004).
At this stage, it is again noted that the ice component of the coupled ice/ocean model which has been configured for this study contains both dynamic (i.e.: relatively short term wind and current influences) and thermodynamic (i.e.: longer term temperature and ice growth influences) aspects. Because of the short time frames (several days) for the hindcast simulations carried out in this study, the thermodynamics of the model have not been included in the model runs, because ice growth is limited over several day periods.

3.2.3 Numerical Grid

The domain of the coupled ice-ocean model that has been configured for use in this study covers a total area of 6,600 km^2 (of water). It extends from Trois-Rivières which lies to the west of the Gros Cacouna location to Rimouski, which is situated to its east. Figure 3.1 shows this model domain with each ten grid cells that have been used in the numerical modelling study overlain on it. The Gros Cacouna site is indicated by the red circle and lies at grid point (333,713)

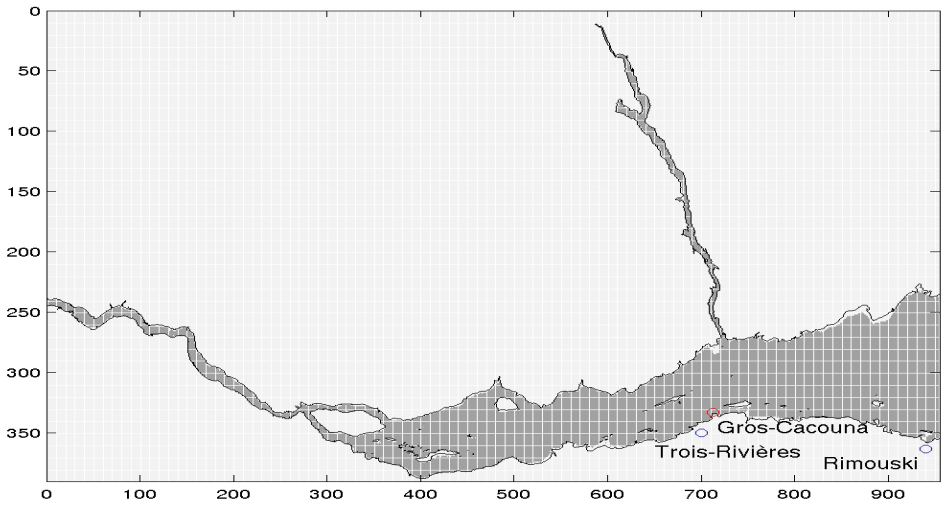

Figure 3.1: Grid of St. Lawrence Estuary model at 400m horizontal resolution.

The horizontal resolution of the grid is 400 m on a Lambert conformal projection, and the vertical resolution in the water column is 5 m in the upper Estuary, upstream from the Saguenay Fjord. The bathymetry of the river bed that is used within the model has been taken from the highest resolution digital marine charts produced for this region by the Canadian Hydrographic Service. The thicknesses of the surface and bottom layers of the water column adjust to the local water level and depth, respectively.

3.2.4 Model Inputs

There are a number of key inputs to the coupled ice-ocean model that drive it. These inputs are briefly highlighted as follows.

Weather Parameters

The atmospheric forcing that is input to the model includes wind fields over its domain at 10m in height, air temperatures and dew point depressions (at a 2m height), precipitation rates and cloud cover fraction. The grid values for these parameters were interpolated in time and space from the analyses produced with the Canadian operational weather forecast model at a 35 km grid resolution. The forecast was based on a regional finite element model prior to February 24, 1997 (Mailhot et al., 1997), and the Global Environmental Multi-scale model thereafter (Côté et al., 1997a and b). This model provides sequential 9-hour forecasts + 12-hour analyses of three-hourly fields of winds, temperatures and so forth, using uninterrupted series of global analyses and the variational method that is in place at the Canadian Meteorological Centre in Montreal.

In the ice hindcasting study carried out here, the atmospheric model was not coupled to an interactive ice-ocean model, as it could be in an ice forecasting application (see Pellerin et al., 2004). Instead, the grid values for the atmospheric parameters needed as input to the hindcast runs were taken directly from existing weather results files. As a detail, it should be noted that the original weather model forecasts from which this input data was obtained made use of surface conditions taken from daily global analyses of sea surface temperatures and sea ice cover observations, and therefore reflect these effects. Also, within the coupled model used here, the ice-ocean, atmosphere-ocean, and ice-atmosphere heat, salt and momentum fluxes are represented with bulk aerodynamic formulae (e.g., Parkinson and Washington, 1979).

River Run-off

River run-off is another input forcing to the ice-ocean model. This input is prescribed as boundary conditions on momentum, temperature (taken as being equal in the neighbouring ocean grid cell), and salinity on the upstream side of the 24 grid cells bounding the estuary. The run-off values are interpolated in time from daily observations (Hydat database, Environment Canada), and normalized to represent the input from the drainage basin. The most important river discharge rate is through the upstream Trois-Rivières section.

3.3 Initial Conditions

The ocean component of the coupled model that has been used in this ice hindcast study is spun up from a state of rest, and temperature and salinity solutions available from a 7 year analysis of the Gulf of St Lawrence, estuary and river areas (Saucier et *al*., in preparation). The ocean then evolves over a spin up period of 24 hours, during which the sea level at the mouth of the estuary is ramping to observed tidal variations. The ocean solution becomes a steady state solution after this time, wherein the tidal, run-off cycles and winds control the variability. The internal physics and boundary conditions of the ocean model then determine the different tidal and baroclinic 3D current regimes in the grid area over the subsequent period, as an output of the model run. The water level is specified at each time step along the open model boundaries using the sea level tidal constituents from the Canadian Hydrographic Service.

After 24 hours, once the ocean component of the model has spun up, the ice component of the coupled model is activated. In this regard, ice concentrations and ice thicknesses information is interpolated onto the 400 m grid from the ice chart files that are available from the Canadian Ice Service (Meteorological Service of Canada). Further forcing functions are also added, including the atmospheric forcing parameters outlined above. The ice component of the model then provides outputs about ice conditions, movements and ice pressures across the grid area based on its internal physics, for the remainder of the model hindcast run (3 days).

Here, it should be noted that the presence of fast ice along the shorelines near Gros Cacouna has also been recognized within the model. This factor was accommodated by extending the shoreline boundaries outwards in the model's grid scheme, to the typical locations where fast ice edges are seen. They include the area just east of Gros Cacouna near Isle Verte and the shallows along the coastline between Cacaouna harbour and Rivières-du-Loup.

3.4 Model Simulation Runs

The coupled ice-ocean model, as configured for use in this study, was applied to conduct a variety of ice simulation runs, with the primary objective of assessing the frequency and nature of ice pressure occurrences in the Gros Cacouna area. In order to develop meaningful statistics about ice pressure events, the model was run in a hindcast mode over a seven year period, from the winter of 1996/97 through the winter of 2002/03. This particular time period was chosen due to the availability of various data files from other lower resolution models (ocean, ice and atmospheric ones) that had already been generated, for use as inputs to the 400m grid scale model runs.

The more severe ice conditions that could give rise to ice pressure occurrences in the area of interest were first identified. The key criterion that was used for this purpose was the presence of high ice concentrations (8 - 9/10^{ths} or more). Clearly, significant ice pressure events would not be experienced in lesser ice coverage situations, due to the "lack of connection" of ice floes within the ice cover.

Existing daily sea ice charts produced by the Canadian Ice Service (CIS) on the basis of the Radarsat satellite images and operational ship and helicopter-based observations by the Canadian Coast Guard were firstly reviewed, to define the time frames when this ice concentration criterion was actually observed. Figure 3.2 shows the ice concentration and mean ice thickness values around the Gros Cacouna site, obtained from the sea ice charts over the 1996/97 to 2002/03 period. From these time series, roughly 100 cases with the highest ice concentrations (≥ 8 - 9/10ths) were ultimately selected for simulation runs with the 400m grid scale ice-ocean model. They are summarized in Table 3.1, along with their dates of occurrence and information about the total ice concentrations, ice concentrations in different ice thickness categories, and the mean wind speeds and directions at the time.

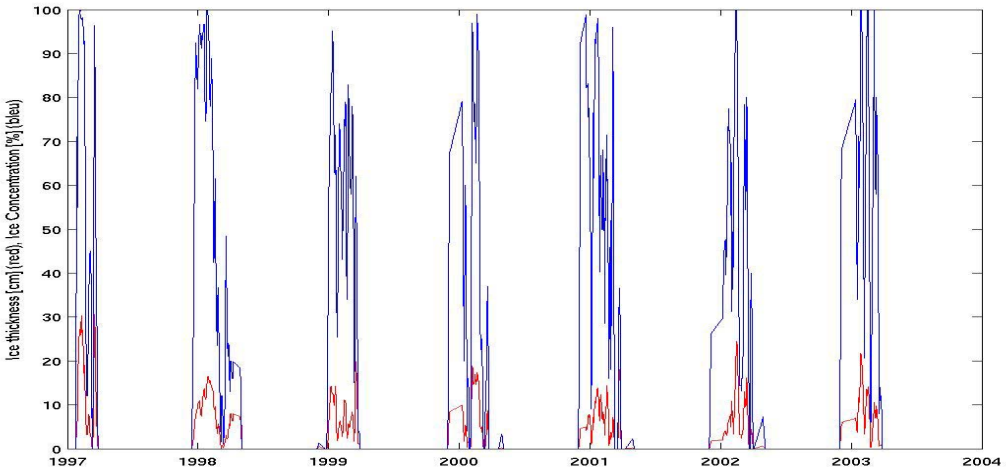

Figure 3.2: Ice concentration and mean ice thickness values near the Gros Cacouna site, over a 7 year period, based on daily sea ice charts produced by the Canada.

Each case was run in a hindcast mode as part of this study, with each run involving a 3 day simulation of ice conditions, movements and possible ice pressure events (excluding the 24 hour spin up period for the ocean model component needed prior to each ice run). Also, the results from the first day of each ice simulation run were not used here, to ensure that its solutions had reached a steady state in the simulations. Hence, two days of relevant ice information was actually generated by each model hindcast run, giving a detailed view of various ice situations over a total time frame of roughly 200 days for the 7 year period considered here.

4. 0 Model Solutions

4.1 General

For the purposes of this study, the key outputs from the ice-ocean model simulation runs that were made are the ice concentration, thickness, movements and internal pressure fields calculated over the model domain, in particular, those seen at the Gros Cacouna site. The thickness and concentration are available as area averages as well as for each thickness category. Concurrent information on parameters such as winds, currents and water levels were also analysed.

In order to focus on the most important ice aspects of the model run results, several basic output products were developed. They are briefly described as follows.

4.2 Time Series Displays

Simple time series displays of the key model output parameters results were generated for each of the simulations run (93 individual cases in total). This was done for the grid point at the Gros Cacouna terminal site.

Figure 4.1 provides an example of one of these sets of time series, in this case for simulation run # 033, which starts on January 23, 1998 at 18:00 hours. The figure contains time series plots for 8 different parameters, including:

IAHI - the mean ice thickness of all of the ice types in the grid cell (cm)

ICON - the mean ice concentration in the grid cell (as a % coverage)
- a value of 90% is equivalent to $9/10^{ths}$, 100% to $10/10^{ths}$, and so forth

IPRS - the ice pressure (or internal isotropic stress) value for the grid cell (Pa)

Wind - a stick plot showing the wind speed (in m/sec) and direction (North is upward)

Current - the mean current speed in the surface water layer of grid cell (m/sec)

Ice Speed - the mean ice drift speed in the grid cell

WLEV - the elevation of the water surface relative to mean sea level (m)
- these values reflect tides, barotropic effects, and so forth

IAHI x IPRS - the line load (or force per horizontal meter) in the ice cover (N/m)
- this value is calculated as the product of the ice pressure and the ice thickness that is present at the time it represents the "constraining" load that a vessel would feel along each meter of its hull length

These basic time series plots have been produced for the Gros Cacouna terminal site, for all of the simulations carried out in this modelling work. A quick review of these time series plots is instructive. For example, they show that ice pressure events are generally cyclical, with relationships to the tidal cycle. They also suggest that ice drift speeds are typically low when ice pressure events occur, which is not surprising. These aspects are discussed later in this report.

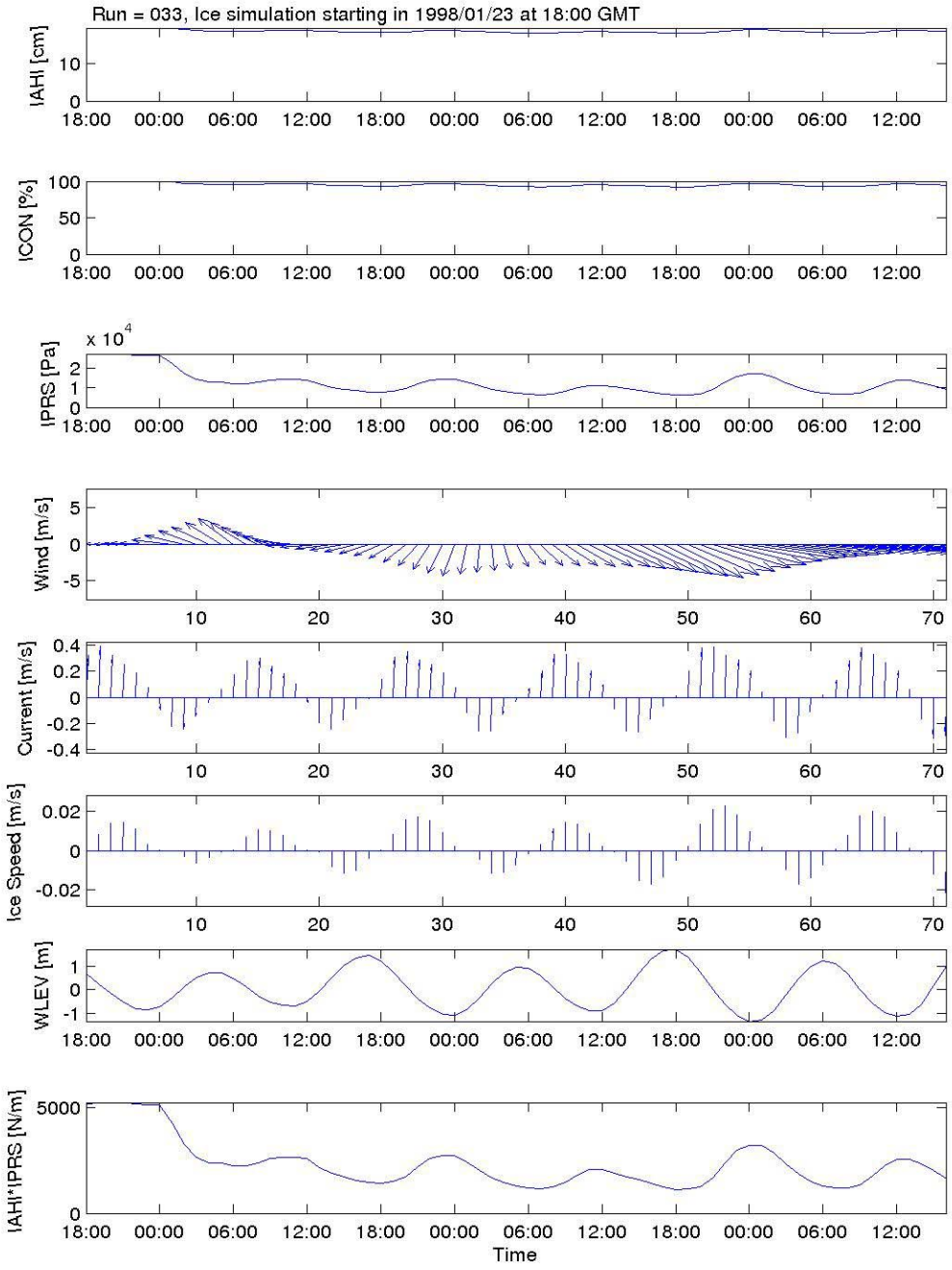

Figure 4.1: Representative time series plots for 8 key parameters, generated from the results of the model. This particular set of time series is for simulation run # 033, which starts at 18:00 on January 23, 1998 and covers a 3 day time period.

5.0 Analysis & Results

5.1 General

The modelling work that has been conducted in this study has generated a vast amount of hincast data about various ice conditions and other environmental factors in the general Gros Cacouna area. As outlined at the beginning of the report, the primary objective of this modelling effort is to provide information about ice pressure occurrences near the proposed terminal site, and specific answers to the following questions.

- How frequent are ice pressure events at the proposed LNG terminal location?
- What is the nature of these ice pressure events (magnitudes, durations, etc.)?
- What are the primary causes of ice pressure (winds, currents, tides, etc.)?

The types of model outputs that were described in the last section have been analyzed to address these key questions. The analysis methods used, and the key results obtained, are outlined in this section of the report.

5.2 Frequency of Ice Pressure Events

5.2.1 Initial Screening

The approach that was adopted in this modelling work was to select roughly 100 cases which had conditions conducive to ice pressure occurrences near the terminal site. The main criterion used to screen out these cases involved the presence of ice concentrations in excess of $8/10^{ths}$ around Gros Cacouna (more specifically, 85% coverage over a 5 km x 5 km grid cell containing the site). The use of this criterion implicitly assumes that ice pressures will not occur when ice concentrations are in the low to moderate range, which is a realistic assumption.

A review of the CIS ice chart data over the 7 winter periods considered in this study (1996/97 to 2002/03) showed roughly 150 time intervals when this criterion was met. Each case typically lasted anywhere from a few hours to a few days (Figure 3.2). This is consistent with separately derived statistics which suggest high ice concentration situations should be expected around the Gros Cacouna site about 30% of the time in winter, on average (Wright and Masterson, 2004).

These 150 cases were further reduced to the 100 most potentially severe cases, again using ice concentrations as the key criterion. Checks that were made of other factors such as wind speeds and directions suggested they were secondary in terms defining potential pressure occurrences. The 100 cases resulting from this next selection step all involved ice concentrations of $9/10^{ths}$ or more as shown Table 3.1. (note: 7 of the cases were not run due to a lack of input wind data).

This screening process basically ruled out the possibility of ice pressure events over considerable parts of each winter, due to the presence of ice concentrations that were insufficient to cause high internal stresses in the ice cover. On the other hand, all of the time periods when the most significant ice pressure events could occur were identified and then used for the model simulation runs. In short, this approach should capture all of the significant ice pressure events near Gros Cacouna over the 7 year period, and provide sound information about pressure event frequencies.

5.2.2 Definition of Thresholds

Any threshold(s) that is used to define "what is a meaningful ice pressure event" is an important consideration in this study. Here, the magnitude of the ice pressure events identified in the model simulations have been equated to the "constraining forces" that may be imposed on a tanker and, in turn, to the ability of one or more support tugs to counteract these forces.
The force that a tanker may experience due to an ice pressure event can be estimated as:

$$F = p \times hi \times Lt$$

where:
p = ice pressure applied globally, due to ice convergence
hi = mean ice thickness in the area
Lt = waterline length of the tanker

For ice pressure events giving rise to internal ice stresses in the range of 20 kPa, and a mean ice thicknesses in the order of 0.3m, this implies an ice pressure related force of about 180 tonnes on a tanker roughly 300m in length. However, in pragmatic terms, the ability of a tug to counteract forces on the tankers they are supporting will likely be in the order of 50 tonnes, once their in-ice propulsion components are considered. This background has been used as the basis for defining the threshold values for significant ice pressure events in this study. This total force equates to an ice line load level (or force per horizontal meter) of 1.67 kN/m. When this threshold value is exceeded in a particular model simulation run, then the time period over which it is exceeded is considered to be a meaningful ice pressure event.

5.2.3 Other Factors

There are two other factors that should be noted here. Firstly, the ice component of the coupled ice-ocean model includes an upper limit on the internal stresses that can be generated in the ice cover. This upper limit has been set at 27.5 kPa, and represents the point at which out-of-plane deformations (i.e.: ridging, rafting and rubbling) are assumed to begin in the model. This value is quite reasonable to use on a mesoscale, over lengths that are in the range of a kilometre. Within the model, ice deformation processes such as ridging are recognized and accommodated by an increase in ice thickness.
Secondly, the ice pressures that have been used in this analysis work were averaged over a 3 x 3 grid cell area (1.2 km x 1.2 km). Although there is not a great deal of variability in ice pressures between contiguous 400m x 400m grid cells, this approach was taken to provide a blended value for the area of marine operations at and near the terminal site.
The nine cells over which the individual ice pressure grid point values from the simulations runs were averaged are shown in Figure 5.2. It may be seen that they encompass the terminal site and the area immediately to its north.

5.2.4 Frequency Statistics

All of the ice pressure values that were generated by the 93 model runs were used to calculate line loads due to internal ice stresses. These values have been spliced together for each of the 7 year periods considered, as shown in Figure 5.1. It should be noted that the blank time periods between the values shown are ones with ice concentrations of $< 9/10^{ths}$, when meaningful ice pressure occurrences are not expected In this figure, the 1.67 kN/m (or 50 tonne) threshold that

has been used to define significant ice pressure events is also shown by the horizontal red lines in the plots.

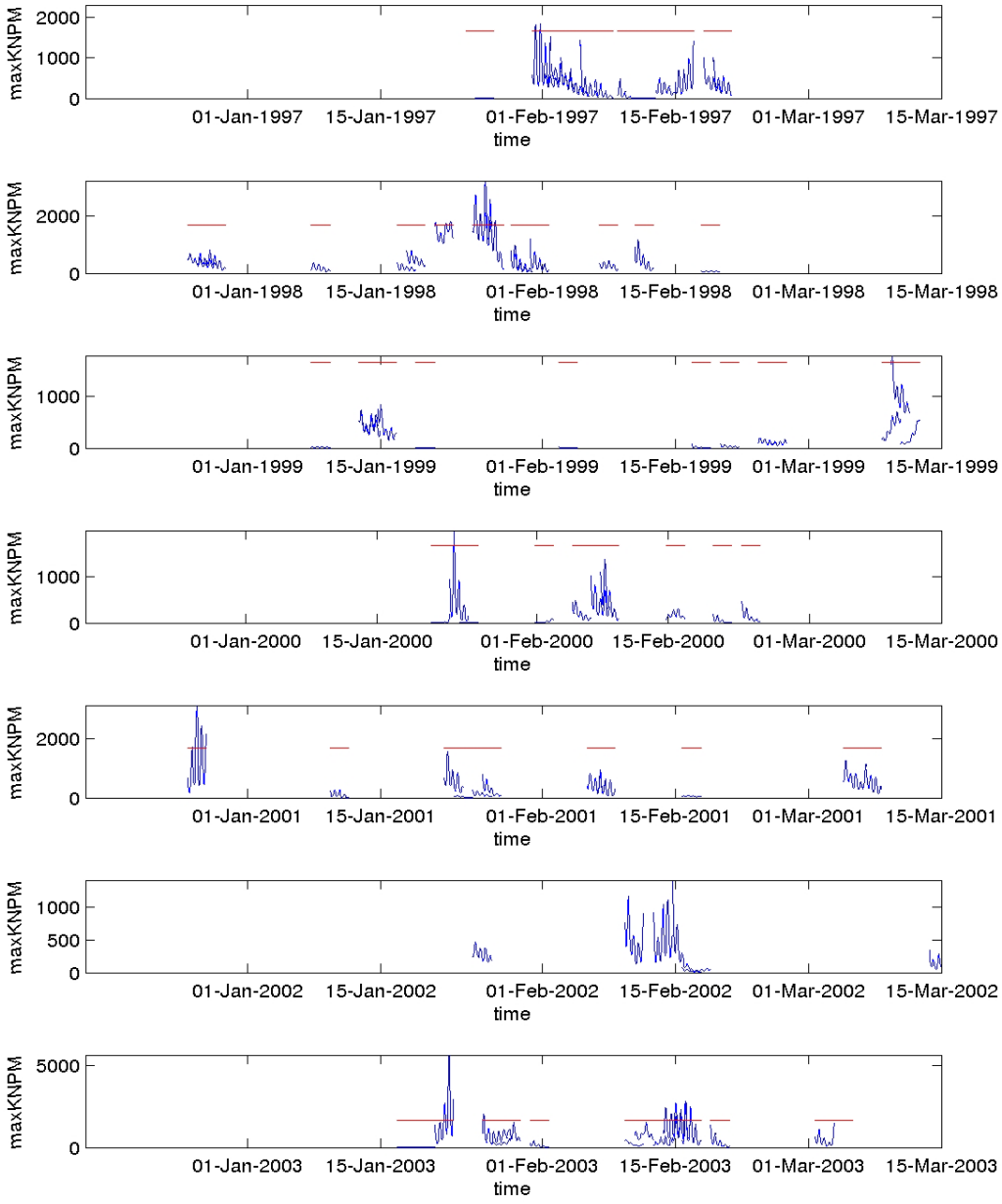

Figure 5.1: Blended time series of the 7 years of ice line load event data (pressure x mean ice thickness) for the terminal site, with the "significant event threshold" of 1.67 kN/m shown by the horizontal red lines. Only the last 48 hours of each simulation run are plotted here.

In total, there are 324 ice pressure events indicated over the 7 winters that are summarized in this figure. However, 299 of these events lie below the 1.67 kN/m threshold value which defines a significant ice pressure occurrence. There are 25 events where the pressures exceed this threshold, but are less than 3.3 kN/m (or 100 tonnes on a tanker, which represents the need for two tugs). One event has a peak value of 5.67 kN/m (which would require four tugs to counteract).

Based on Figure 5.1, the high degree of inter-annual variability that should be expected in the number of ice pressure events at Gros Cacouna is clear, with most events being seen over the mid January to mid March time frame. Over the seven year period, there are 25 ice pressure events, suggesting an average event frequency of several per year (i.e.: 25/7). However, there were no significant ice pressure events hindcast during the winter of 2002, while there were 9 in 2003. Table 5.1 provides a summary of the number of ice pressure events that have been predicted by this modelling study over the 7 year period.

Table 5.1: Inter-annual variability in the number of ice pressure events hindcast by year

Year	Number of high pressure events
Winter 1996-1997	3
Winter 1997-1998	8
Winter 1998-1999	1
Winter 1999-2000	1
Winter 2000-2001	3
Winter 2001-2002	0
Winter 2002-2003	9
Average	3.57

5.3 Characteristics of Ice Pressure Events

5.3. 1 Durations

The next question that was considered is "how long do these significant ice pressure events last". To address this question, the ice pressure (ice line load) time series were reviewed to determine the duration of each of the 25 hindcasted ice pressure events. The resultant duration data was then plotted in the form of a cumulative exceedence graph, which is shown in Figure 5.2.

Based on this figure, it can be seen that significant ice pressure events are generally short, ranging from several hours to half a day. The median and 90% non-exceedence values for the duration of an ice pressure event are 6 hours and 8 hours, respectively.

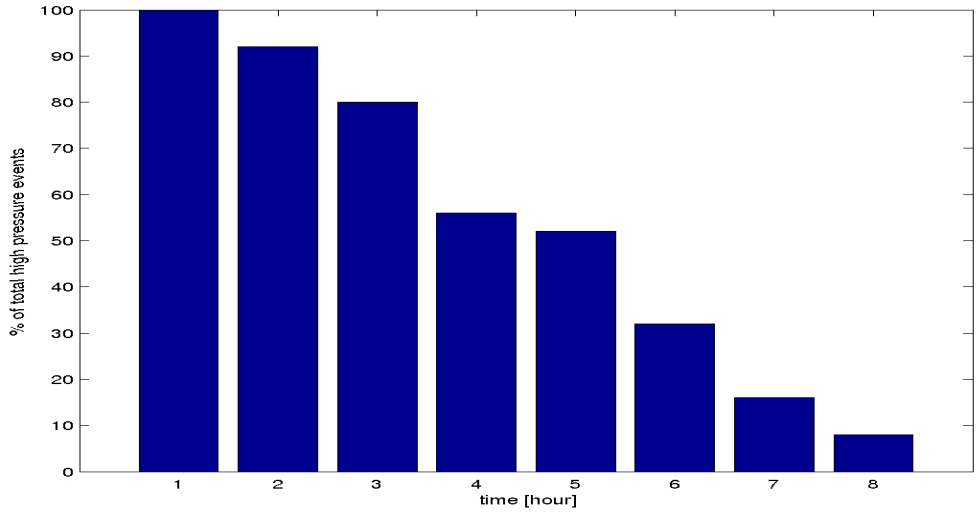

Figure 5.2: Cumulative exceedence plot for the duration of significant ice pressure events.

Here, it should also be noted that many of the ice pressure events identified by the model runs are nearly contiguous in time, with the values of ice line load falling below the significance threshold for a few hours, and then increasing again. Recognizing this aspect, the overall duration of events wherein the ice pressure levels rise and fall over short time frames have also been estimated. For this purpose, a time period of up to 12 hours has been "allowed" between those time periods with load levels exceeding the significance threshold value of 1.67 kN/m. This procedure has the effect of reducing the number of (individual) ice pressure events (per year) but increasing their overall (or grouped) durations. Figure 5.3 provides a cumulative exceedence plot for the 8 significant ice pressure events that have been defined in this manner. For this grouped pressure event case, the median and 90% non-exceedence duration values are 4 hours 24 hours, respectively.

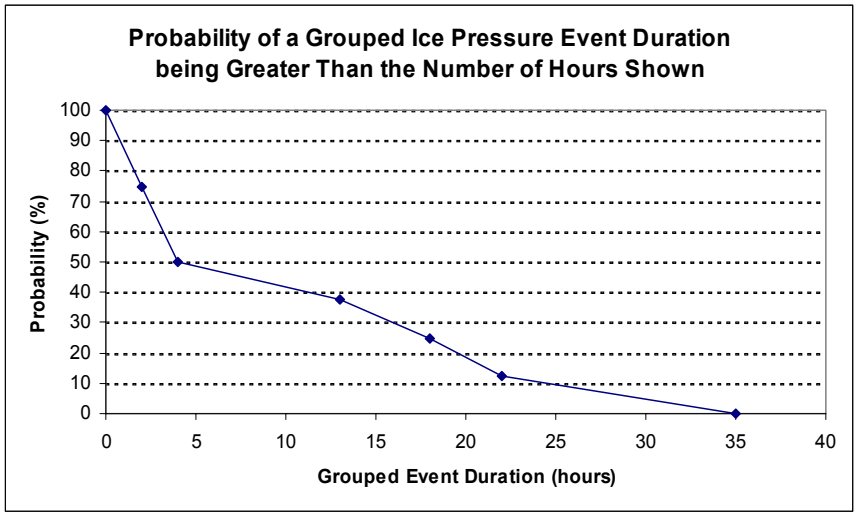

Figure 5.3: Cumulative exceedence plot for the duration of grouped ice pressure events.

5.3.2 Frequency of events

A quantitative analysis of the time intervals between significant ice pressure event sequences has not been undertaken in this study, largely due to the low frequency of occurrence of these events. Here, the main point to make is that they are typically long, in the range of many days to many weeks. This can be seen in Figure 5.1, where only a handful of significant ice pressure events are suggested in most years, ones that are often "bunched together" in time. As noted earlier, no significant ice pressure occurrences were identified by this hindcasting study during the winter of 2001/02.

5.3.3 Spatial structures

A Representative example of map display graphic is given in Figure 5.4. That example has also been taken from simulation run # 033, which starts on January 23, 1998 at 18:00 hours and continues for 3 days. In the figure that is shown here, the map graphics are cover the time period from the 49th to the 71st hour after initialization of the ice model run, again at 2 hour intervals. The Gros Cacouna site is in the lower central part of each map, just to the southwest of Isle Verte. The coloured horizontal scale at the bottom of each map (which is dynamic) can be used to get some feel for the magnitude of the particular parameter.

To get some feel for the spatial distribution of ice pressures in the general Gros Cacouna area, the mean values of all of the ice pressures produced by the 93 model simulation runs were plotted in map form. The result is given in Figure 5.5, where mean ice line loads from all of the hindcast runs are shown for a sub-region around the terminal site. The 9 grid cells over which ice pressures and line loads were averaged for parts of the ice pressure event assessment study are also shown, with the terminal site located in the lower central cell. The land is depicted by dark red, the fast ice by red, and the shoreline by the black line.

Although this figure provides a mean view of the ice pressure distribution that is averaged over time, it shows a clear gradient in internal ice stresses, due to ice convergence against the shoreline and fast ice boundary. Figure 5.6, which shows the spatial distribution of ice pressure during the most severe event (run # 033), is also included here for interest. It indicates a similar gradient in ice pressures with distance offshore. In terms of causes of significant ice pressure events, these figures suggest that proximity to the shoreline or fast ice edge is an important determinant.

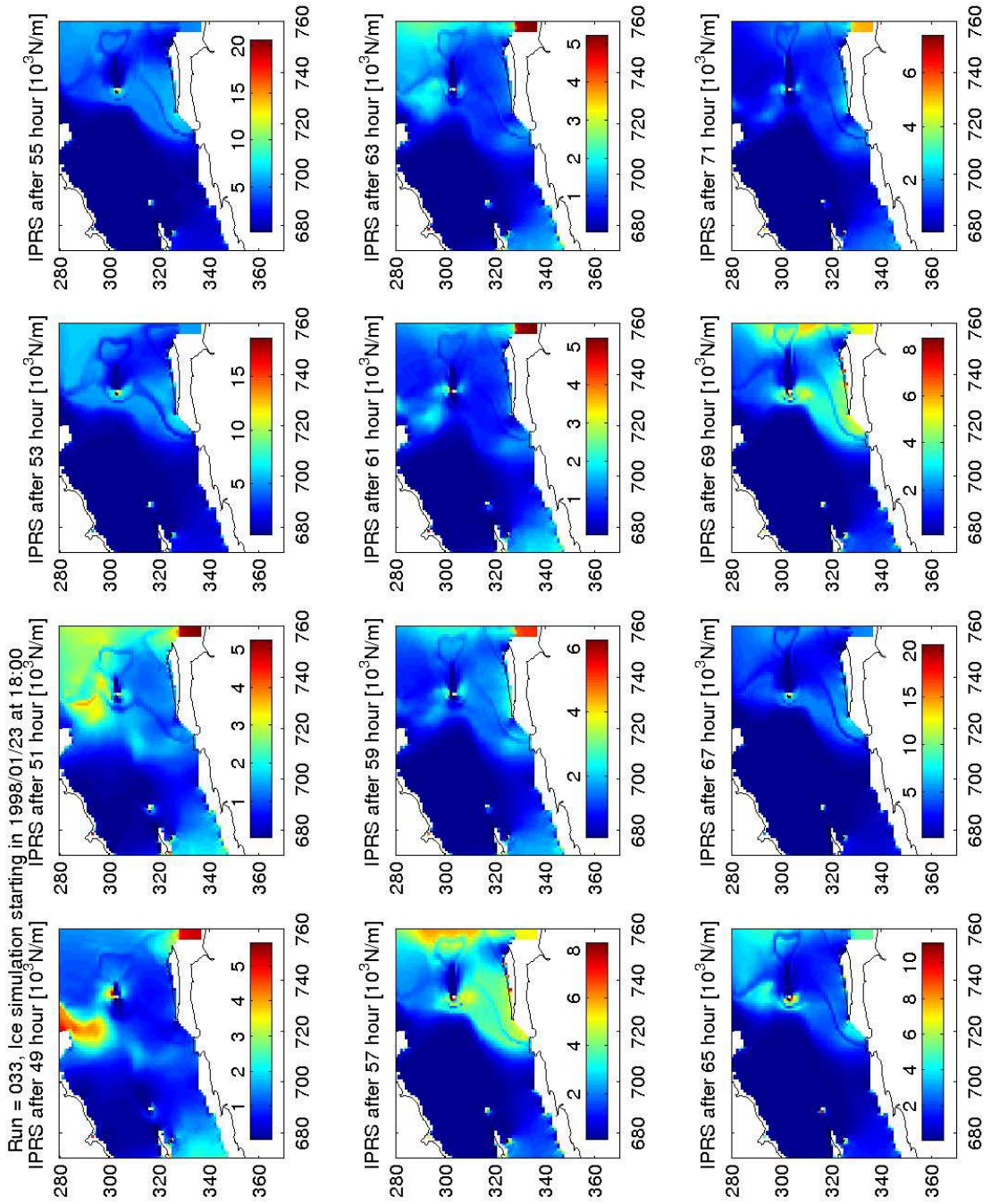

Figure 5.4:Horizontal force of the ice [N m^{-1}] over the map area for the 49th to the 71st hour after the initialisation of the ice model simulation (run 033).

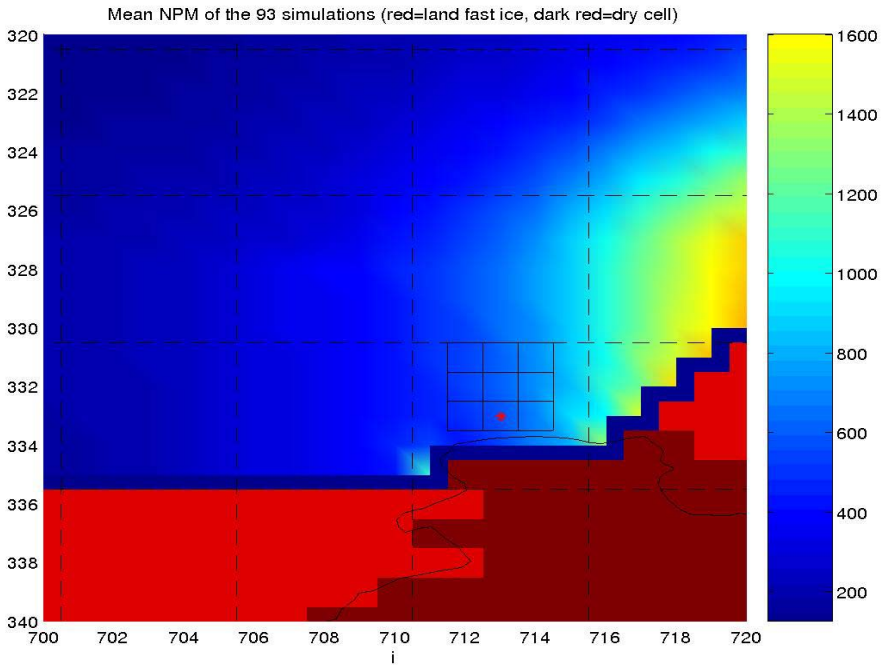

Figure 5.5: A map of the region around the proposed Gros-Cacouna terminal site, with the land shown in dark red, the fast ice in red, and the coastline by the black line. The mean ice pressure value (expressed as the ice line load in Nm-1) is depicted here. The pressure values are averaged over the 93 simulations, and cover the 7 winter periods from February 1997 to March 2003. The red dot indicate the location of the terminal site.

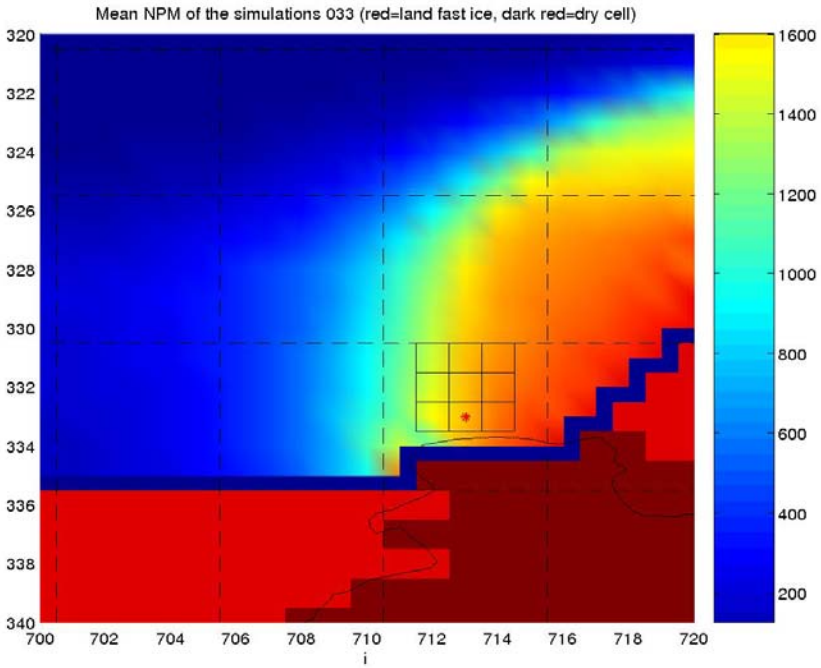

Figure 5.6: Similar map of the ice pressure distribution in the Gros cacouna area to that shown above, in this case, for a significant ice pressure event identified in simulation run # 033.

5.4 Causes of Ice Pressure Events

The main causes of significant ice pressure events around the Gros Cacouna terminal site were also investigated as part of this study. The 25 key events that were identified as exceeding the 1.67 kN/m threshold in the model simulation runs are summarized in Table 5.2, together with concurrent ice, current and wind parameter data. The following observations can be made on the basis of a cursory review of this information.

- All of the significant ice pressure events occur when ice concentrations are very high, with ice coverage values that are in the range of 95% or more
- Although the largest ice pressures are not necessarily associated with the highest mean ice thicknesses, the largest ice line loads generally are (since these ice line loads are the product of the ice pressure and the ice thickness)
- When significant ice pressure events occur, ice drift speeds are generally very low, in the range of 1 cm/sec in most cases (if not stationary).
- Over the 1.2 km x 1.2 km scale for the ice pressure values considered in this study, about one quarter of the identified events involve ice pressures close to the 27.5 kPa limit, where active ridging and rubbling within the ice cover can be anticipated.
- Many of the significant ice pressure events appear to occur when the current flow is down the river, with a component towards the river's southern shoreline

Although wind speeds and directions do not appear to have a dominant effect, some of the higher ice pressure values are associated with strong winds out of the northwest.

Table 5.2: Data associated with the 25 significant ice pressure events identified over 7 years.

#	Thickness (cm)	Ice Conc. (%)	IPRS (Pa)	Curr. (ms^{-1})	Curr. Dir. (°N)	Ice speed (ms^{-1})	Ice Dir. (°)	Wind (ms^{-1})	Wind Dir. (°N)	KNPM (Nm^{-1})
1	16,67	0,96	13703	0,145	40,93	0,007	50,68	4,54	139,40	2283,76
3	23,29	0,93	7825	0,115	69,21	0,008	61,60	2,29	-48,30	1822,83
3	23,28	0,93	7917	0,200	46,24	0,016	51,22	3,14	-45,89	1842,93
31	18,11	0,95	9763	0,193	33,19	0,009	34,14	3,01	-114,54	1767,99
31	18,38	0,94	9446	0,087	53,32	0,002	52,41	7,17	131,32	1735,76
31	18,48	0,95	9746	0,211	28,03	0,008	35,52	4,88	130,31	1800,80
33	18,78	0,97	14451	0,216	29,33	0,012	40,12	4,07	-163,37	2713,94
33	18,49	0,95	11183	0,126	38,63	0,004	58,27	5,03	128,12	2068,15
33	18,93	0,97	17030	0,227	28,31	0,014	45,27	7,40	104,97	3223,75
33	18,75	0,96	13637	0,230	28,77	0,013	45,91	7,43	98,86	2557,49
34	19,66	0,94	9369	0,185	28,07	0,012	40,71	4,83	96,19	1841,91
67	14,30	0,96	12565	0,172	40,68	0,009	33,69	4,45	174,41	1796,91
75	10,49	0,96	19005	0,128	50,87	0,008	82,32	7,09	114,46	1994,38
94	11,10	0,97	15262	0,186	-170,47	0,007	-173,66	6,97	115,26	1694,48
94	11,70	1,00	26590	0,389	-170,18	0,025	-159,75	8,90	114,20	3111,58

94	11,43	0,98	21110	0,048	116,16	0,002	87,48	6,25	105,10	2412,16
129	22,32	0,96	12206	0,303	-170,66	0,008	-166,22	10,10	89,81	2724,32
129	23,30	0,99	24342	0,124	43,17	0,007	60,46	10,65	101,78	5671,17
131	21,45	0,94	9628	0,104	53,86	0,007	60,98	4,01	25,75	2064,87
140	10,50	0,99	23375	0,172	39,04	0,014	39,40	5,53	86,56	2454,78
140	10,38	0,98	19949	0,077	77,71	0,003	80,76	8,11	103,00	2071,26
140	10,62	1,00	25726	0,132	47,19	0,013	45,06	7,45	108,29	2732,75
140	10,52	0,99	21999	0,098	156,54	0,001	103,76	7,13	112,87	2313,25
141	10,27	1,00	27500	0,071	62,79	0,009	69,67	8,56	126,13	2825,62
141	10,16	0,99	24737	0,132	48,45	0,009	59,16	6,73	119,70	2512,55

To assess the possible causes of ice pressure events in more detail, output data from all 93 of the model simulation runs was used, not only the event cases exceeding the significance threshold. For this purpose, scatter plots were produced between the ice line load values from the hindcast results and concurrent environmental factors. These scatter plots are shown in Figure 5.7 below. In these plots, a horizontal red line has also been included to indicate the threshold for a pressure event that is of significance for marine operations around the terminal.

Some of these scatter plots do not suggest any strong relationships between the occurrence of ice pressure events and the particular parameter shown. However, they do indicate that significant ice pressure events are usually associated with the presence of high ice concentrations, the low water and currents occurring during ebb tides, and strong wind occurrences from the northwest.

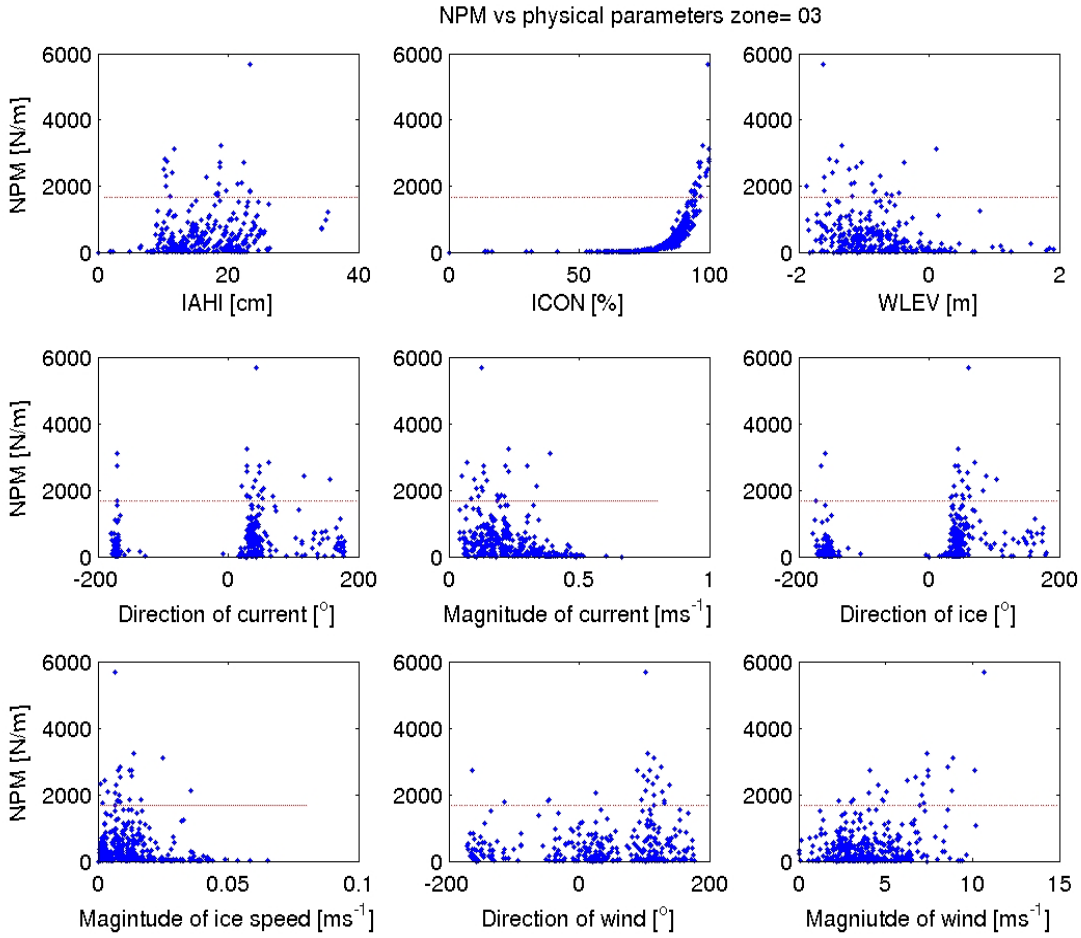

Figure 5.7: Scatter plots of ice pressure (ice line load) values against various physical parameters, including mean ice thickness, ice concentration, water level, current direction, current speed, ice drift direction, ice drift speed, wind direction and wind speed.

6.0 Conclusions

Highly variable and at times severe winter ice conditions in the Estuary and Gulf of St. Lawrence represent an important constraint for ship transits and operations. Strong tidal currents and synoptic meteorological events continuously redistribute the drifting pack ice cover and produce internal ice pressure events on time scales of few hours, and spatial scales of few kilometres. Although a reasonable level of information about ice conditions around Gros Cacouna is now available, no information about the occurrence of ice pressure events near the terminal site was available prior to this study.

In order to estimate the recurrence time and controlling factors for ice pressure events near Gros Cacouna, the dynamics of severe ice condition events were examined using a high-resolution 3D coupled ice-ocean numerical model of the St. Lawrence Estuary. This model is based on state-of-the-art physics, accounts for ocean currents, ice dynamics, and wind stresses. The ocean

component of the model was already validated for the Estuary, while the ice component and flux-coupling schemes to the ice had been implemented and tested for other regions.

Internal ice pressure events can be seen when ice concentrations are high, and the ice cover cannot accommodate convergence without an internal build-up of stress. In this study, approximately 100 cases were selected from a 7 year period (1996/97 to 2002/03) when the observed large scale ice concentrations exceeded 85%. These cases were examined by simulating ice dynamics in the general Gros Cacouna area with the high-resolution ice-ocean model applied in a hindcast mode. These simulations involved more than 400 days of computer time. For each simulation case run, the evolving ice pressure field was examined over a several day period as a function of the "forcing" environmental parameters, and the spatial and temporal distribution of ice pressure events determined.

The key conclusions of this study are summarized as follows.

(1) High ice pressure events occur when the ice concentrations observed on scales of several km exceed 95%, generally during ebb tide currents and north-westerly winds, which tend to confine the drifting pack ice cover against the shoreline (and local fast ice edges). The internal ice pressure generally relaxes during semi-diurnal tidal flood currents.

(2) Over the 7 year period that was analyzed, 25 significant ice pressure events were identified at the Gros Cacouna terminal site, which gives an average of about 3.5 events per winter. These pressure events occurred intermittently over the mid-January to mid-March time frame, with anywhere between 0 and 9 events identified per winter. Typical event durations were in the range of 6 hours, with extreme event durations in excess of a day.

(3) Given the accuracy of weather information and the ice-ocean prediction model, ice conditions near the Gros Cacouna site are highly predictable over time scales of few hours to few days. Hence, ice pressure events can be predicted to support of marine operations at and around the terminal site in the future, by applying the type of model used here in a forecast mode.

In addition to ice pressure information, this study has also produced concurrent time series of relevant ice, ocean and weather parameters in the area of interest over a 7 year period, on short time scales and small spatial scales. Although it is a by-product of the study, this information can be used for other purposes, for example, in future operational assessments, for the development of statistics, and so forth.

7.0 References

Atakturk SS, Katsaros KB (1999) Wind stress and surface waves observed on lake Washington. J Phys Oceanogr, 29:633-650

Backhaus JO (1983) A semi-implicit scheme for the shallow water equations for application to shelf sea modeling. Cont Shelf Res 2: 234-254

Backhaus JO (1985) A three-dimensional model for the simulation of shelf-sea dynamics. Dtsch Hydrogr Z 38:165-187

Bignami F, Marullo S, Santoreli R, Schiano ME (1995) Longwave radiation budget in the Mediterranean Sea. J Geophys Res 100:2501-2514

Boer GJ, Flato GM, Ramsden D (2000) A transient climate change simulation with greenhouse gas and aerosol forcing: projected climate change in the 21st century. Clim Dyn 16:427-450

Burchard, H, Bolding K (2001) Comparative analysis of four second-moment turbulence closure models for the oceanic mixed layer. J Phys Oceanogr 31:1943-1968

Canuto VM, Howard A, Cheng Y, Dubovikov MS (2001) Ocean turbulence, I, One-point closure model: Momentum and heat vertical diffusivities. J Phys Oceanogr 31:1413-1426

Charnock H (1955) Wind stress on a water surface. Q J R Meteorol Soc 81:639-640

Côté J, Gravel S, Méthot A, Patoine A, Roch M, Staniforth A (1997a) The operational CMC/MRB Global Environmental Multiscale (GEM) model: Part I - Design considerations and formulation. Mon Weather Rev 126:1373-1395

Côté J, Gravel S, Méthot A, Patoine A, Roch M, Staniforth A (1997b) The operational CMC/MRB Global Environmental Multiscale (GEM) model: Part II – Results. Mon Weather Rev 126:1397-1418

Cox M (1984) A primitive equation, three-dimensional model of the ocean. GFDL Ocean Group Tech. Report No. 1, GFDL/NOAA Princeton 143 pp.

Fissel, D., K. Borg, E. Ross and R. Birch (2005) Ice Thickness and Velocity at Gros Cacouna, St. Lawrence River, December 2004 to April 2005. ASL report prepared for submission to Trow Engineering.

Hunke EC, Dukowicz JK (1997) An Elastic-Viscous-Plastic Model for Sea Ice Dynamics. J Phys Oceanogr 27: 1849-1867

Hunke EC (1998) CICE : the Los Alamos Sea Ice Model Documentation and Software User's Manual, T-3 Fluid Dynamics Group, Los Alamos National Laboratory, Los Alamos, NM 87545

Idso SB, Jackson RD (1969) Thermal radiation from the atmosphere. J Geophys Res 74:5397-5403

Kantha LH, Mellor GL (1989) A two-dimensional coupled ice-ocean model of the Bering Sea marginal ice zone. J Geophys Res 94:10921-10935

Kantha LH., Clayson C.A (1994) An improved mixed layer model for geophysical applications. J Geophys Res 99: 25235-25266.

Koutitonsky, V. (2005) Monitoring Ice Conditions at Gros Cacouna Using Time Lapse Digital Photography. UQR-ISMER report submitted to B. Wright & Associates Ltd.

Koutitonsky, V.G. , Saucier, F.J., Senneville, S., and Guyondet (2005) T. Three-dimensional tidal currents distributions around the Gros Cacouna LNG ship terminal in Eastern Canada. Report submitted to Sandwell Inc.

Laevastu T (1960) Factors affecting the temperature of the surface layer of the sea. Comm Phys Math 25:1-136

Large WG, Pond S (1982) Sensible and latent heat flux measurements over the ocean. J Phys Oceanogr 12:464-482

Loder, JW, Petrie B, Gawarkiewicz G (1998) The coastal ocean off northeastern North America: a large-scale view. Ch.5 In: The Sea vol. 11 John Wiley & Sons p.105-133

Mailhot J, Sarrazin R, Bilodeau B, Brunet G, Pellerin P (1997) Development of the 35-km version of the operational regional forecast system. Atmos-Ocean 35:1-28

Mellor GL, Yamada T (1982) Development of a turbulence closure model for geophysical fluid problems. Rev. Geophys. Space Phys 20 (4): 851-875

Mellor GL, Kantha LH (1989) An ice-ocean coupled model. J Geophys Res 94:10937-10954

Milko R (1986) Potential ecological effects of the proposed Grand Canal Diversion project on Hudson and James bays. ARCT 39(4):316-326

Padman L, Kottmeier C (2000) High-frequency ice motion and divergence in the Weddell Sea. J Geophys Res 105:3379-3400

Parkinson CL, Washington WM (1979) A large-scale numerical model of sea ice. J Geophys Res 84:311-337

Pellerin, P., Ritchie, H., Saucier, F.J., Roy, F., Desjardins, S., Valin, M., Lee, V. (2004) Impact of a two-way coupling between an atmospheric and ocean-ice model over the Gulf of St. Lawrence. Monthly Weather Review, 132(6), 1379-1398.

Saucier, F.J. et Chassé, J. (2000) Tidal circulation and buoyancy effects in the St. Lawrence Estuary, Canada, Atmosphere-Ocean 38 (4): 1-52.

Saucier, F.J., Chassé, J., Couture, M., Dorais, R., D'Astous, A., Lefaivre, D. et Gosselin, A. (1999) The making of a surface current atlas of the St. Lawrence Estuary, Canada, Fourth international conference on computer modelling of seas and coastal regions (C. A. Brebbia & P. Anagnostopoulos, Eds.) J. Computational Mechanics, Wessex Institute of Technology Press, 87-97.

Saucier, FJ, Dionne J (1998) A 3D coupled ice-ocean model applied to Hudson Bay, Canada: The seasonal cycle and time-dependent climate response to atmospheric forcing and runoff. J Geophys Res 103: 27689-27705

Saucier FJ, Roy F, Gilbert D, Pellerin P, Ritchie H (2003) The formation and Circulation Processes of Water Masses in the Gulf of St. Lawrence. J Geophys Res 108: 3269-3289

Semtner AJ.Jr (1976) A model for the thermodynamic growth of sea ice in numerical investigations of climate. J Phys Oceanogr 6:379-389

Smagorinsky J (1963) General circulation experiments with primitive equations. I. The basic experiment. Mon Weather Rev 91(3):99-164

Stronach JA, Backhaus JO, Murty TS (1993) An update on the numerical simulation of oceanographic processes in the waters between Vancouver Island and the mainland: the GF8 model. Oceanogr Mar Biol Ann Rev 31: 1-86

Thorndike AS, Rothrock DA, Maykut GS, Colony R (1975) The Thickness Distribution of Sea Ice. J Geophys Res 80:4501-4513

Unesco (1981) Algorithms for computation of fundamental properties of seawater, UNESCO Tech Pap Mar Sci 4: 53 p

Wright, B. and D. Masterson (2004) A Summary of Ice Conditions at the Gos cacouna Terminal Site and in the Gulf of St. Lawrence. Report submitted to TPL.

Wright, B. and J. Tseng (2005) Ice Observations Taken During a Field Reconnaissance Trip to the Proposed Gros Cacouna Terminal Site on February 24th, 2005. Report submitted to TCPL.

Wright, B. Analysis of Ice Conditions from Time Lapse Video Records Obtained at Gros Cacouna over the Winter of 2004/05. Report submitted to TCPL.

Zalesak ST (1979) Fully multidimensional flux-corrected transport algorithms for fluids. J Comput Phys 31: 335-362

Zillman, JW (1972) A study of some aspects of the radiation and heat budgets of the southern hemisphere oceans. Meteorol Study Report 26, Bur. Meteorol., Dept. of the Interior Canberra Australia 526